

Optical Doppler Tomography

Zhongping Chen, Yonghua Zhao, Shyam M. Srinivas, J. Stuart Nelson, Neal Prakash, and Ron D. Frostig

(Invited Paper)

Abstract—Optical Doppler tomography (ODT) is an imaging modality that takes advantage of the short coherence length of a broad-band light sources to perform micrometer-scale, cross-sectional imaging of tissue structure and blood flow dynamics simultaneously. We review in this paper the principal of ODT and its applications. Results from *in vitro* and *in vivo* model studies demonstrated that ODT can map the blood flow velocity profile with high spatial resolution in scattering medium. ODT detection mechanisms are illustrated using Monte Carlo simulations. The application of ODT to image brain hemodynamics is demonstrated. Finally, we discuss the limitations of the current technology and application of a phase resolved technique to improve image speed and quality.

Index Terms—Biomedical image, Doppler flowmetry, optical Doppler tomography, optical coherence tomography.

I. INTRODUCTION

DIRECT VISUALIZATION of tissue anatomy and physiology provides important information to the physician for diagnosis and management of disease. High spatial resolution noninvasive techniques for imaging *in vivo* tissue structure and blood flow dynamics are currently not available as a diagnostic tool in clinical medicine. Such techniques could have a significant impact on biomedical research and patient treatment for diseases having a vascular etiology or component. In dermatology, for example, the superficial dermal plexus alone is particularly affected by the presence of disease (e.g., psoriasis, eczema, scleroderma), malformation (e.g., port-wine stain, hemangioma, telangiectasia), or trauma (e.g., irritation, wound, burn). In these situations, it would be most advantageous to the clinician if blood flow and structural features could be isolated and probed at user-specified discrete spatial locations in either the superficial or deep dermis. Localized blood flow monitoring is also critical for reconstructive procedures involving rotational or free flaps where vascular occlusion occurs in 5%–10% of cases [1]. Early recognition of vascular compromise is essential for the salvage of failing flaps and replants because the effectiveness of intervention is inversely related to the duration of ischemia

Manuscript received March 10, 1999. This work was supported by the Whitaker Foundation under Grant 23281ZC and by the Institutes of Arthritis and Musculoskeletal and Skin Diseases under Research Grant AR43419. Institutional support from the Office of Naval Research under Contract N00014-94-1-0874, by the National Institutes of Health under Grant RR-01 192, the Department of Energy under Contract DE-FG03-91ER61227, and by the Endowment at the Beckman Laser Institute and Medical Clinic.

Z. Chen, Y. Zhao, S. M. Srinivas, and J. S. Nelson are with the Beckman Laser Institute, University of California at Irvine, Irvine, CA 92612 USA.

N. Prakash and R. D. Frostig are with the Department of Psychobiology, University of California at Irvine, Irvine, CA 92612 USA.

Publisher Item Identifier S 1077-260X(99)07524-3.

[1]. It is known that the microvasculature of mammary tumors has several distinct differences from normal tissues. Three-dimensional (3-D) mapping of the vasculature may provide new information to discriminate between benign and malignant tumors.

Currently, techniques such as Doppler ultrasound (DUS) and laser Doppler flowmetry (LDF) are used for blood flow velocity determination. DUS is based on the principle that the frequency of ultrasonic waves backscattered by moving particles is Doppler shifted. However, the relatively long acoustic wavelengths required for deep tissue penetration limit the spatial resolution of DUS to approximately 200 μm . Although LDF has been used to measure mean blood perfusion in the peripheral microcirculation, high optical scattering in biological tissue limits spatial resolution.

Localized flow velocity determination with high spatial resolution can be achieved using coherence gating. Our group, and others, have developed a noninvasive technique, optical Doppler tomography (ODT) [2]–[5], for quantitative blood flow measurement with high spatial resolution. In this paper, we first describe the principle of ODT. Results from *in vitro* and *in vivo* model studies will then be presented. ODT detection mechanisms are illustrated using Monte Carlo simulations. The application of ODT to image brain hemodynamics is demonstrated. Finally, limitations of the current technology and application of a phase resolved technique to improve image speed and quality are discussed.

II. OPTICAL DOPPLER TOMOGRAPHY

ODT is based on optical coherence tomography (OCT), an imaging modality that takes advantage of the short coherence length of broad-band light sources to perform micrometer-scale (μm), cross-sectional imaging of biological tissues [5]–[8]. ODT combines LDF with OCT to obtain high resolution tomographic images of static and moving constituents simultaneously in highly scattering biological tissues. Using a Michelson interferometer with a low coherence light source, ODT measures the amplitude and frequency of the interference fringe intensity generated between reference and target arms to form structural and velocity images. High-spatial resolution is possible because light backscattered from the sample recombines with that from the reference beam and forms interference fringes only when the optical path length difference is within the source coherence length. When light backscattered from a moving constituent interferes with the reference beam, the detected

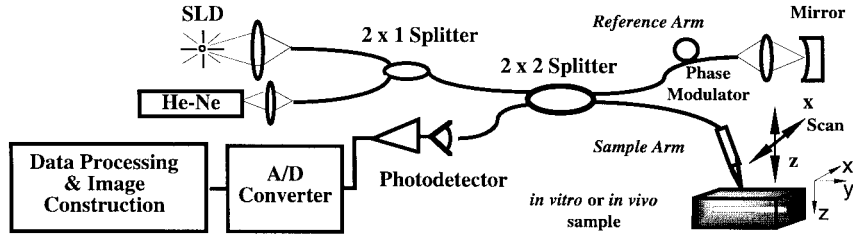


Fig. 1. Fiber-based ODT system.

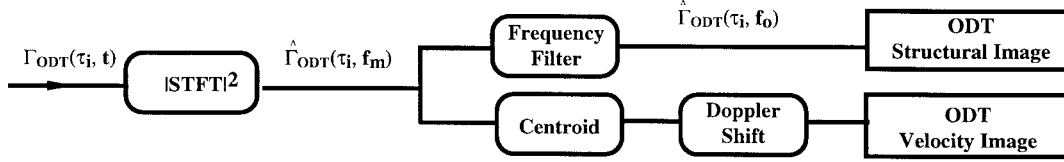


Fig. 2. Signal processing algorithms to obtain ODT structural and velocity images.

temporal interference fringe $\Gamma_{\text{ODT}}(t)$ is given by

$$\Gamma_{\text{ODT}}(t) = A(t) \cos(2\pi(f_0 - \Delta f_D)t + \phi(t)) \quad (1)$$

where $A(t)$ is the amplitude modulation due to tissue inhomogeneity, and $\phi(t)$ is the phase term that depends on the path length difference between reference and sample arms and the intrinsic backscatter spectrum. f_0 is the phase modulation frequency of the interferometer, and Δf_D is the Doppler frequency shift due to the moving scatterers

$$\Delta f_D = \frac{1}{2\pi} (\mathbf{k}_s - \mathbf{k}_i) \cdot \mathbf{v} \quad (2)$$

where \mathbf{k}_i and \mathbf{k}_s are wave vectors of incoming and scattered light, respectively, and \mathbf{v} is the velocity of the moving particle. With knowledge of the angle between $(\mathbf{k}_s - \mathbf{k}_i)$ and \mathbf{v} , measurement of Δf_D allows the particle velocity to be determined at discrete user-specified locations in turbid samples.

III. METHOD

Fig. 1 shows the experimental set up of an ODT system using a fiber optic Michelson interferometer with a superluminescent diode (SLD) as the light source ($\lambda_o = 850$ nm, $\Delta\lambda_{\text{FWHM}} = 25$ nm). Light from the SLD and an aiming beam (He-Ne laser, $\lambda = 633$ nm) are coupled into a fiber interferometer using a 2×1 coupler and then split equally into reference and target arms by a 2×2 fiber coupler. Piezoelectric cylinders are used to modulate the optical path length difference of light in the reference and target arms by stretching the fiber wrapped around the cylinders. A ramp electrical wave (80 Hz) is used to drive the piezoelectric cylinders to generate optical phase modulation for the interference fringes ($f_o = 1600$ Hz). Light in the sample path is focused onto the turbid sample by a gradient index lens (NA = 0.2) with the optical axis oriented at 15° from the surface normal. ODT structural and velocity images are obtained by sequential lateral scans of the sample probe (i.e., fiber tip and gradient index lens) at constant horizontal velocity (800 $\mu\text{m/s}$) followed by linear incremental movement along the surface normal.

To maintain the coherence gate at the beam waist position in the turbid sample, a dynamic focus-tracking technique

is used, where for each incremental movement (δ_1) of the sample probe along the surface normal, the reference mirror is translated (δ_2) to compensate for the new beam waist position. By requiring the coherence gate to be at the beam waist position, a relationship between δ_1 and δ_2 is derived from geometrical optics [2]

$$\delta_2 = \delta_1(\bar{n}^2 - 1) \quad (3)$$

where \bar{n} is the mean refractive index of the turbid sample. Dynamic focus-tracking not only maintains lateral spatial resolution when probing deeper positions, but also increases the signal-to-noise ratio (SNR).

Light backscattered from the turbid sample is coupled back into the fiber and forms interference fringes at the photodetector. $\Gamma_{\text{ODT}}(t)$ is measured by a single element silicon photovoltaic detector, where t is the time delay between light from the reference and sample arms, and is related to the optical path length difference (ΔL) by $t = \Delta L/c$. High axial spatial resolution is possible because interference fringes are observed only when t is less than the source coherence time τ_c or, equivalently, when ΔL is less than the source coherence length ($L_c = \tau_c c$). The interference fringe intensity signal is amplified, band passed, digitized (20 kHz) with a 16-bit analog-to-digital (A/D) converter, and transferred to a computer workstation for data processing. Signal processing algorithms to obtain structural and velocity images from recorded temporal interference fringe intensities are illustrated in Fig. 2.

Time-frequency analysis is used to calculate the Doppler shift. The power spectrum of the temporal interference fringe at the i th pixel corresponding to time delay τ_i in the structural and velocity images is calculated by a short-time Fourier transformation (STFT)

$$\hat{\Gamma}_{\text{ODT}}(\tau_i, f_m) = |\text{STFT}(f_m; \Gamma_{\text{ODT}}(\tau))|^2 \quad (4)$$

where f_m is the discrete frequency value. A tomographic structural image is obtained by calculating the value of the power spectrum at the phase modulation frequency (f_o). Because the magnitude of the temporal interference fringe

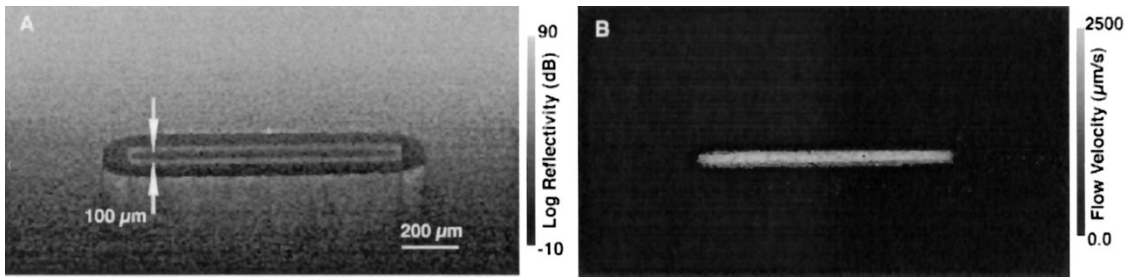


Fig. 3. ODT structural (A) and velocity (B) images of flowing intralipid in a rectangular glass conduit with inner dimensions of $100 \times 2000 \mu\text{m}$ submerged 1 mm below the surface in a turbid sample of intralipid. The arrows indicate the inner conduit dimension.

intensity decreases exponentially with increasing depth in the turbid sample, a logarithmic scale (5) is used to display the ODT structural images

$$S_{\text{ODT}}(i) = 10 \cdot \log(\hat{\Gamma}_{\text{ODT}}(\tau_i, f_o)) \quad (5)$$

Fluid flow velocity is determined from the Doppler frequency shift (Δf_D), which is the difference between the carrier frequency established by the optical phase modulation (f_o) and the centroid (f_c) of the measured power spectrum at the i th pixel

$$v_{\text{ODT}}(i) = \frac{\lambda_o \Delta f_D}{2\pi \cos(\theta)} = \frac{\lambda_o (f_c - f_o)}{2\pi \cos(\theta)} \quad (6)$$

where we have assumed, $\mathbf{k}_s = -\mathbf{k}_i$ and θ is the angle between \mathbf{k}_i and \mathbf{v} (2). The centroid of the measured power spectrum is determined by

$$f_c = \frac{\sum_m f_m \hat{\Gamma}_{\text{ODT}}(\tau_i, f_m)}{\sum_m \hat{\Gamma}_{\text{ODT}}(\tau_i, f_m)} \quad (7)$$

Lateral and axial spatial resolutions are limited by the beam spot size and source coherence length (L_c), to 5 and 13 μm , respectively; higher axial resolution may be achieved using a low coherence source with greater spectral bandwidth. Velocity resolution (100 $\mu\text{m/s}$) is dependent on pixel acquisition time (Δt_p) and the angle (θ) between flow velocity (\mathbf{v}) and the incoming light direction (\mathbf{k}_i) in the turbid sample; velocity resolution may be improved with a smaller angle (θ) or longer pixel acquisition time (Δt_p).

IV. RESULTS AND DISCUSSION

A. *In vitro* and *in vivo* Images

To demonstrate potential applications of ODT for imaging blood flow, *in vitro* and *in vivo* models were investigated. In the *in vitro* model, a small rectangular cross section glass conduit was submerged 1 mm below the surface of a highly scattering 1% intralipid solution. ODT structural [Fig. 3(A)] and velocity [Fig. 3(B)] images were obtained when a suspension of 1% intralipid was infused through the conduit at constant velocity by a linear syringe pump. Although scattering from 1% intralipid was high ($\mu_s = 23 \text{ cm}^{-1}$) and the conduit was invisible to the unaided eye when viewed from the top surface of the phantom, both the conduit and flowing intralipid are observed, respectively, in ODT structural and velocity images. In the ODT structural image [Fig. 3(A)], the gray scale change

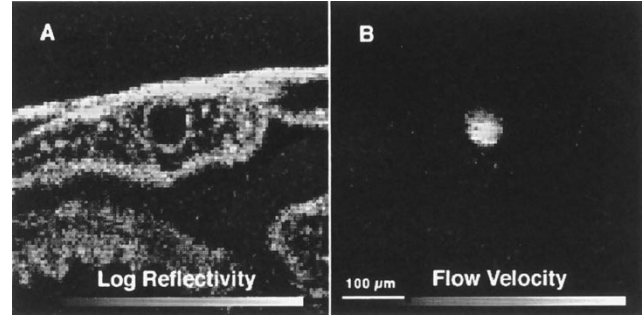


Fig. 4. ODT structural (A) and velocity (B) images of aortic blood flow in *Xenopus laevis*.

from white at the surface to darker shades at deeper locations indicates strong attenuation of the temporal interference fringe intensity due to scattering in the turbid sample. In the velocity image [Fig. 3(B)], static regions in the conduit appear dark ($V = 0$), while the presence of intralipid moving at different velocities with maximum flow velocity along the central axis is evident.

In the *in vivo* model, morphology and blood circulation of *Xenopus laevis* tadpoles were imaged (Fig. 4). Morphologies of the aorta was evident in the structural image [Fig. 4(A)]. High-contrast imaging of aortic blood flow velocity is shown in Fig. 4(B). These results demonstrate that ODT can image tissue structure and blood flow simultaneously with high spatial resolution at discrete user-specified locations in a biological tissue.

B. Monte Carlo Simulations of ODT

Imaging *in vivo* blood flow using ODT requires a detailed understanding of light propagation in a medium containing moving red blood cells (RBC) buried in a turbid sample. Although results from our *in vitro* and *in vivo* models clearly demonstrate that flow can be imaged using ODT, the effects of many factors, such as flow velocity, particle concentration, vessel diameter, tissue scattering parameters, and detector configuration on image quality, have not been investigated. Inasmuch as the scattering mean free path in blood is less than 10 μm , the detected photons are bound to undergo multiple scattering events, even from the smallest blood vessels. It is not difficult to construct examples from nonuniform (e.g., parabolic) velocity fields for laminar flow in a cylindrical vessel, where the total Doppler shift shown by a photon that undergoes two scattering events will be very different from

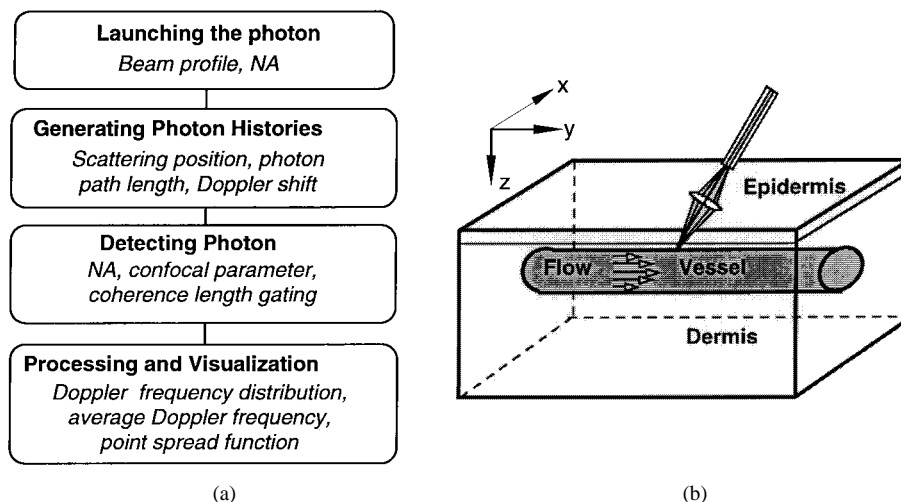
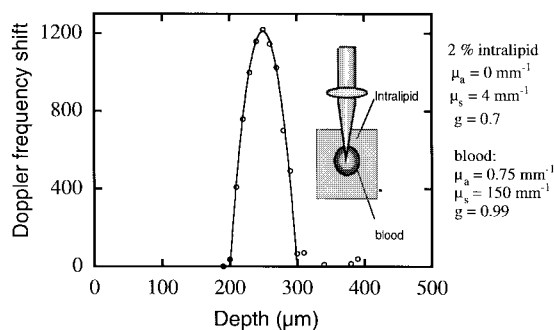


Fig. 5. Monte Carlo simulation modules.

Fig. 6. Average Doppler frequencies for photons detected through a 100- μm diameter vessel placed at a depth of 250 μm in 2% intralipid solution.

the exact value reported from a single backscattering event. Furthermore, the point spread function will be further degraded due to multiple scattering.

We have developed a Monte Carlo method to simulate photon propagation and investigated the effects of multiple scattering and other factors on ODT image quality to provide guidance for further system optimization [9], [10]. The simulations have been designed such that different parameters can be investigated from a photon history file generated from a single Monte Carlo simulation. The simulation is divided into four modules: launching of photons, generation of photon histories, detection of photons with coherence gating, and processing and visualization [Fig. 5(a)]. The physical model comprises a vessel surrounded by a scattering medium, which consists of intralipid for *in vitro* studies, and epidermal and dermal layers for human skin for *in vivo* studies [Fig. 5(b)]. A parabolic velocity profile is assumed for blood flow in small vessels.

Fig. 6 shows the average Doppler frequencies for photons detected as the focus of the probe is moved along the z axis. The velocity distribution in the 100 μm diameter vessel located 250 μm below the surface is taken from the parabolic profile for laminar flow with a maximum velocity of 2 mm/s. Although the photon undergoes multiple scattering events in the vessel before being backscattered to the probe, the Doppler frequency shift from the simulation (circles) agrees with the theoretically expected values (solid line) determined from the specified parabolic velocity profile.

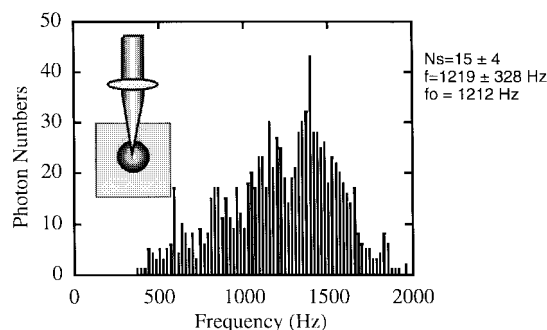


Fig. 7. Frequency spectrum of detected photons when the probe focuses in the center of the vessel.

The frequency spectrum of the detected photons when the probe focuses in the center of the vessel is shown in Fig. 7. The average number of scattering events (N_s) that each photon undergoes before being detected is 15. Although the frequency spectrum is very broad, the mean value is 1219 Hz, which is very close to the mathematically expected value of $f_o = 1212$ Hz. This is a significant finding considering the fact that each photon undergoes more than 10 scattering events and the Doppler spectrum of the detected photon has a standard deviation of 328 Hz. Closer examination of the individual histories for photons backscattered from the central region of flow reveals that each photon experiences a series of stochastic small angle forward scattering events on the downward path through the vessel, a backscattering in the central region of the vessel, and a series of small angle forward scattering events on the upward path through the vessel. Because the Doppler frequency shift is proportional to the change in the scattering wave vector ($\mathbf{k}_s - \mathbf{k}_i$), forward scattering is responsible for the broadening of the Doppler spectrum. Therefore, averaging of Doppler frequencies over many photons for each focus position very accurately approximates the true frequency.

C. Applications of ODT

The noninvasive nature and exceptionally high spatial resolution of ODT have distinct applications in the clinical

management of patients in whom imaging tissue structure and monitoring blood flow dynamics is essential.

- Provide a *in situ* (3-D) tomographic image and velocity profile of blood perfusion in human skin at discrete spatial locations in either the superficial or deep dermis.
- Monitor the effects of pharmacological intervention on skin microcirculation (e.g., effects of vasoactive compounds or inflammatory mediators; determination of transcutaneous drug penetration kinetics; evaluation of the potency of penetration enhancers; irritation of chemical compounds, patch-test allergens and ultraviolet radiation; comparison of the reactivity of the skin microcirculation in different age and ethnic groups).
- Diagnosis and treatment of tumors in the gastrointestinal and respiratory tracts, cervix, and skin.
- Map 3-D tumor microvasculature for angiogenesis research [11]–[13].
- Determine burn depth (provide guidance regarding the optimal depth for burn debridement prior to definitive closure).
- Monitor tissue perfusion and viability immediately after injury, wound closure, replantation, or microvascular reconstruction.
- Optimize radiation dosimetry by assessing and quantifying alterations in tissue microvascular and matrix structure.
- Determine long-term alterations in microvascular hemodynamics and morphology in chronic diseases such as diabetes mellitus and arteriosclerosis.
- Map cortical hemodynamics with high spatial resolution for brain research.
- Image flow dynamics in the microchannels of microelectromechanic system (MEMS) chips.

We have demonstrated that ODT can be used for vasoactive drug screening [14], and for monitoring intratumoral blood flow during photodynamic therapy (PDT) [14]. Photocoagulation of blood vessels with pulsed dye laser has been investigated with ODT [15]. Cardiac dynamics in embryos have been imaged with ODT [16]. In the following section we discuss another important application of ODT: imaging cortical blood flow for brain research.

The cerebral cortex is generally believed to be composed of functional units called “columns,” that are arranged in clusters perpendicular to the surface. Each column is comprised of neurons that respond preferentially to a specific feature of a stimulus that differs from its neighboring columns. Furthermore, perpendicular to functional columns and parallel to the surface, the cortex is composed of six anatomical “layers,” with layer I being the outermost and VI the innermost. Each anatomic layer is different by virtue of its connectivity pattern and/or cellular composition. Throughout the cortex, capillaries form a dense network near neurons. Changes in brain blood flow are known to be coupled to regions of neuronal activity. However, it is poorly understood whether there are layer differences in blood flow changes that occur within a column. Changes in blood flow within a cortical column are clinically important because disruption of this

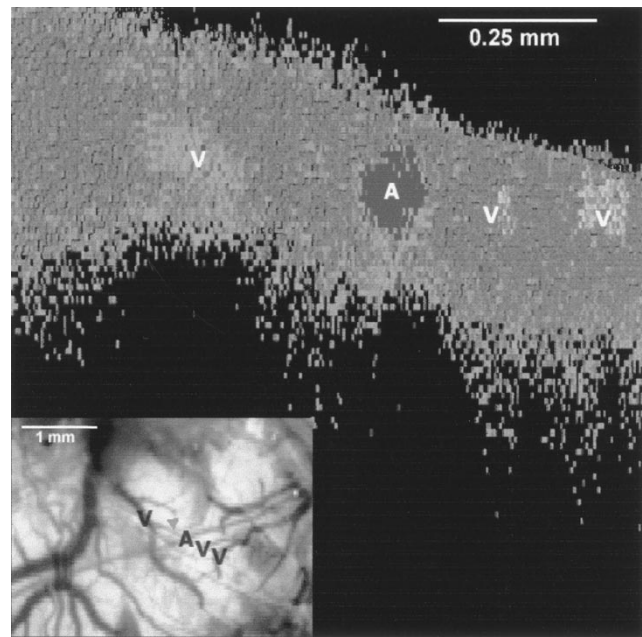


Fig. 8. ODT image of blood flow in the rat cerebral cortex.

coupling is likely related to certain types of neuropathology, such as dementia [17].

Several different techniques have been used to study the coupling of blood flow within localized regions of brain activity, such as Positron Emission Tomography (PET), Near Infrared Spectroscopy, Blood-Dye Imaging, Intrinsic Signal optical Imaging (ISI), Laser Doppler Perfusion Imaging (LDPI), functional Magnetic Resonance Imaging (fMRI), and two photon microscopy. High spatial resolution, on the order of micrometers, is necessary to distinguish different vascular components (arterioles, capillaries, venules) and individual columns, which are about 100–200 square micrometers in tangential size. The current resolutions of PET, LDPI, and fMRI are too low to distinguish these components. Although ISI can map out *en face* cortical hemodynamics and columns, depth resolution is not available [18]. Two photon microscopy has been used for mapping cortical activity. However, flow measurement requires fluorescent dye injection, which can be problematic, if the objective is to image blood flow changes induced by pharmacological agents [19]. The noninvasive high resolution tomographic capabilities of ODT make it a promising technique for mapping depth resolved cortical blood flow.

To evaluate the potential of ODT to measure cortical blood flow, the cerebral cortex of an anesthetized rat was imaged through a dural incision. The rat's head was stabilized from unwanted motion using a stereotactic apparatus. Fig. 8 shows an ODT image of *in vivo* blood flow in the upper layers in the rat cerebral cortex. The cortical surface is shown at the top of the image. The colored pixels (blue and red/yellow) denote regions of flow in opposite direction. The red line in the inset depicts the surface projection of the region of cortex imaged. Note the correspondence of arteries (A) and veins (V) in the inset with the blue and red pixels in the ODT image. Smaller vessel are also visible as discrete blue pixels.

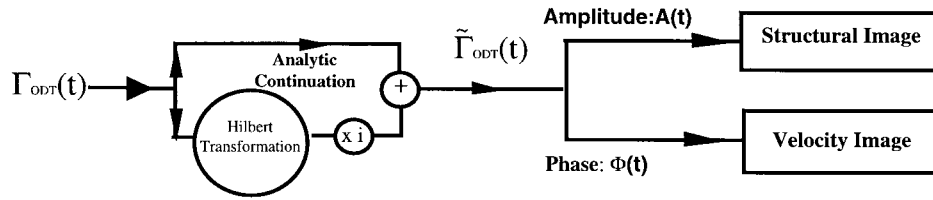


Fig. 9. Schematic diagram of the image reconstruction algorithm for phase resolved ODT.

These preliminary findings demonstrated that ODT can map cortical blood flow with high axial resolution. Although depth is currently limited due to the wavelength of the source used, an imaging depth of about 1 mm could be achieved using a longer probing wavelength, such as 1300 nm [20]. Furthermore, 3-D data may be acquired by multiple two-dimensional (2-D) scanning or by using a tandem array of sensors. ODT shows great promise in brain research for imaging stimulus-induced blood flow changes occurring in all layers of the cerebral cortex with micrometer resolution and without dyes.

D. Phase Resolved ODT

Current ODT is limited by the fact that the image acquisition time is on the order of minutes, which is too long for clinical applications. There are two factors that limit the speed. First, the scanning of the delay line uses mechanical linear translation, which limits speed. Recent development of a rapid-scanning optical delay (RSOD) line based on phase ramp in the optical spectrum domain has overcome this limitation. Second, flow velocity images are reconstructed using spectrogram calculated from the power spectrum with STFT. There are two disadvantages when using a spectrogram for velocity determination. The first disadvantage is that the noise from the power spectrum is always positive, which creates a bias when using the centroid method to determine the Doppler frequency shift [5], [14]. The limited bandwidth tends to underestimate the velocity when the SNR is small. The second disadvantage comes from the conflict between spatial resolution and velocity sensitivity. When STFT is used to calculate flow velocity, accuracy is determined by the window size of the Fourier transformation for each pixel [5], [14]. Inasmuch as detection of the Doppler shift using STFT requires sampling the interference fringe intensity over at least one oscillation cycle, the minimum detectable Doppler frequency shift, Δf_D , varies inversely with STFT window size (i.e., $\Delta f_D \approx 1/\Delta t_p$). With a given STFT window size, velocity resolution ($v_{ODT(\min)}$) is given by

$$v_{ODT(\min)} = \frac{\lambda_o}{2n \cos(\theta) \Delta t_p}. \quad (8)$$

Because pixel acquisition time is proportional to the STFT window size, the image frame rate is limited not only by detector sensitivity, but also by velocity sensitivity. For example, to achieve a velocity sensitivity of 1 mm/s, the minimum acquisition time for each pixel is approximately 0.9 ms, and a full-frame ODT image with 100×100 pixels requires 9 s assuming no overlap in the STFT window. Furthermore, spatial resolution, Δx_p , is proportional to STFT window size

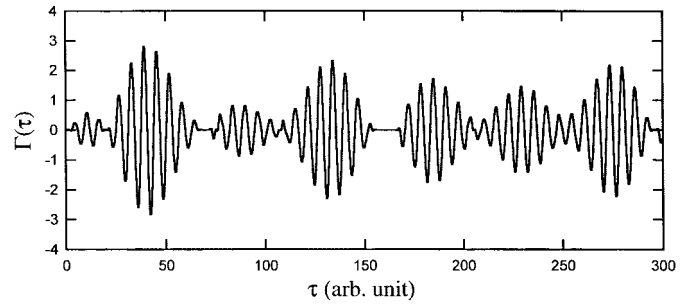


Fig. 10. Typical interference fringe signal used in our phase resolved ODT simulation studies.

and given by

$$\Delta x_p = v \Delta t_p \quad (9)$$

where v is the one-dimensional (1-D) scanning speed of the ODT system. Therefore, a large STFT window size increases velocity sensitivity while decreasing spatial resolution.

There are a number of signal processing techniques that can overcome the limitation of STFT method. We discuss in the following section a phase resolved ODT system that uses phase information for tomographic image reconstruction of flow.

In our current ODT system, the temporal interference fringe intensity ($\Gamma_{ODT}(\tau)$) first undergoes STFT to obtain the power spectrum; the centroid method is then used to calculate the Doppler shift. In phase resolved ODT, the complex valued analytic continuation of the interference fringe function is first determined using Hilbert transformation; the amplitude and phase information are then used to reconstruct structural and velocity images. The schematic diagram for the image reconstruction algorithm is shown in Fig. 9. The complex valued interference fringe function, $\tilde{\Gamma}_{ODT}(\tau)$, is determined through analytic continuation of the measured interference fringes, which can be accomplished by a Hilbert transformation [21]

$$\tilde{\Gamma}_{ODT}(\tau) = \Gamma_{ODT}(\tau) + \frac{i}{\pi} P \int_{-\infty}^{\infty} \frac{\Gamma_{ODT}(\tau')}{\tau' - \tau} d\tau' \quad (10)$$

where P denotes the Cauchy principal value taken at $\tau' = \tau$.

The amplitude $A(\tau)$ and phase $\Phi(\tau)$ of $\tilde{\Gamma}_{ODT}(\tau)$ can then be calculated. The amplitude is then used to reconstruct the structural image. If there is flow in the sample being imaged, the phase change provides velocity information because of the Doppler frequency shift. The derivative of the phase is then used to reconstruct the velocity image. Because the amplitude and phase information can be determined simultaneously for each sampling point of the A/D converter, the velocity at each sampling point can be calculated and the accuracy of the Doppler frequency shift will not be limited by the STFT

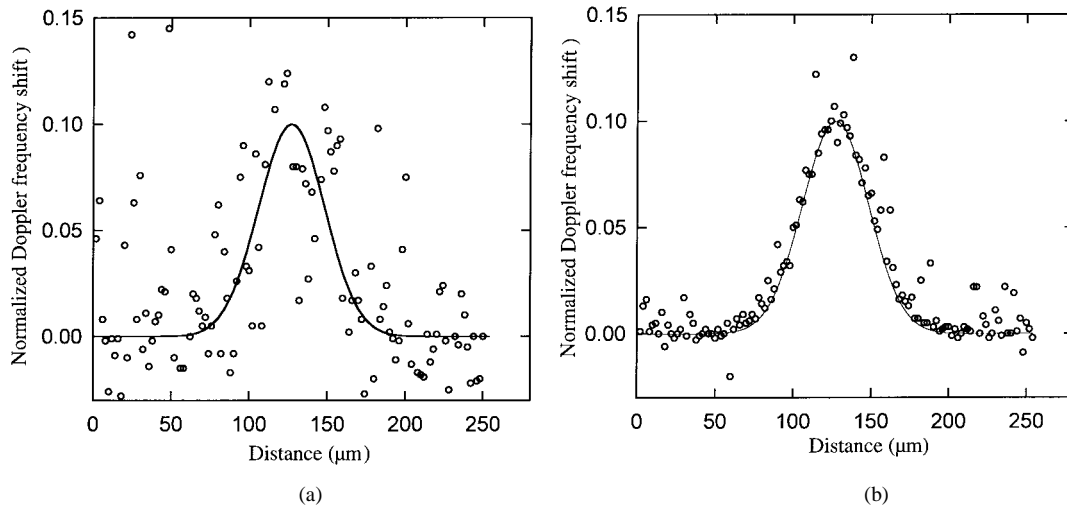


Fig. 11. Velocity profiles reconstructed from the simulation data with (a) power spectrum method using STFT; and (b) phase resolved method using Hilbert transformation. Open circles in the diagrams are simulated results and solid lines the input velocity profiles.

window size of individual pixels. Consequently, phase resolved ODT has decided advantages over existing methods for imaging tissue structure and blood flow with high resolution and high speed.

We have performed several computer simulations to compare the phase resolved and power spectrum methods. The interference fringe signal generated from flow with a Gaussian velocity profile (centered at τ_0 , width b) was simulated as

$$\Gamma_{\text{ODT}}(\tau) = A(\tau) \cos(\Phi(\tau) + \omega_0\tau) \quad (11)$$

where $\Phi(\tau)$ is given by

$$\frac{d\Phi(\tau)}{d\tau} = a\omega_0 e^{(\tau-\tau_0/b)^2} \quad (12)$$

where ω_0 is the carrier frequency generated by phase modulation, and a denotes the ratio of the Doppler frequency shift to the carrier frequency at the peak of the velocity profile. A typical interference fringe signal is shown in Fig. 10. Random discontinuity at zero crossing was included in the fringe signal to simulate the optical statistical properties of particles in the flow and tissue, such as speckle induced signal fluctuations [22]. Using the power spectrum method for flow velocity determination, the simulation result is shown in Fig. 11(a). The velocity profile reconstructed using the phase resolved method under the same conditions is shown in Fig. 11(b). Our simulation results indicate that the phase resolved method gives much higher accuracy in reconstructing the velocity profile as compared to that using the power spectrum. When the Doppler frequency shift is as low as 1% of the carrier frequency, the phase resolved method can easily reconstruct the velocity profile. The minimum velocity that can be resolved by phase determination is a factor of 10 smaller than that using the power spectrum.

To confirm our simulation results, *in vitro* flow measurements were performed on a model phantom system that consisted of a 300- μm lumen diameter plastic tube submerged in 0.1% intralipid gel. Intralipid solution at a concentration of 0.2% was injected through the tube with an average flow velocity of 50 $\mu\text{m/s}$. The angle between the probing beam

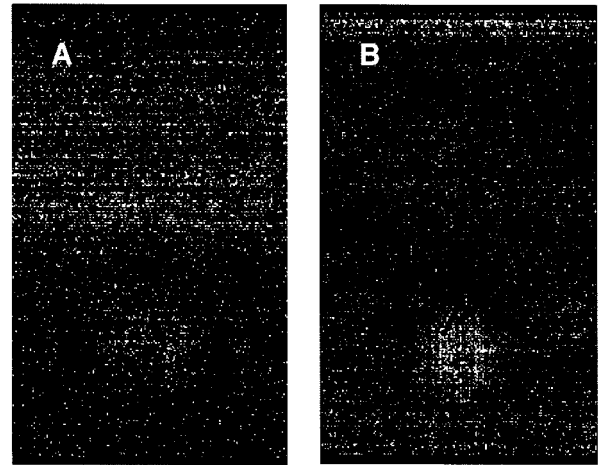


Fig. 12. Velocity images reconstructed from (A) power spectrum method and (B) phase resolved method.

and flow direction was 75° . The carrier frequency of the fringe signal was 8.3 kHz and the Doppler frequency shift induced due to flow was less than 1% of the carrier frequency. Fig. 12(A) shows the velocity image using the power spectrum method. The image shown in Fig. 12(B) was reconstructed using the phase resolved method. The experimental results demonstrated that the phase resolved method can measure the velocity flow profile much more accurately than the power spectrum method.

V. CONCLUSION

ODT is a noninvasive and noncontact optical technique to image tissue structure and blood flow dynamics simultaneously with high spatial resolution. *In vitro* and *in vivo* measurements, as well as Monte Carlo simulation have demonstrated that ODT can map the velocity profile with high precision in scattering medium. Although image speed is currently limited, our results indicate that phase resolved ODT can improve imaging speed. Given the noninvasive nature of the measurement, exceptional spatial resolution, simple hardware requirements, and relatively compact size, ODT is a promising technique for both basic research and clinical medicine.

ACKNOWLEDGMENT

The authors would like to thank T. E. Milner for his contribution in the early phase of ODT development, T. L. Lindmo and D. J. Smithies for their contribution in the Monte Carlo simulation.

REFERENCES

- [1] H. Furnas and J. M. Rosen, "Monitoring in microvascular surgery," *Ann. Plastic Surg.*, vol. 26, pp. 265–273, 1991.
- [2] Z. Chen, T. E. Milner, D. Dave, and J. S. Nelson, "Optical Doppler tomographic imaging of fluid flow velocity in highly scattering media," *Opt. Lett.*, vol. 22, pp. 64–66, 1997.
- [3] Z. Chen, T. E. Milner, S. Srinivas, X. J. Wang, A. Malekafzali, M. J. C. van Gemert, and J. S. Nelson, "Noninvasive Imaging of *in vivo* blood flow velocity using optical Doppler tomography," *Opt. Lett.*, vol. 22, pp. 1119–1121, 1997.
- [4] J. A. Izatt, "In vivo bidirectional color Doppler flow imaging of picoliter blood volumes using optical coherence tomography," *Opt. Lett.*, vol. 22, pp. 1439–1441, 1997.
- [5] M. D. Kulkarni, T. G. van Leeuwen, S. Yazdanfar, and J. A. Izatt, "Velocity-estimation accuracy and frame-rate limitations in color Doppler optical coherence tomography," *Opt. Lett.*, vol. 23, pp. 1057–1059, 1998.
- [6] D. Huang, E. A. Swanson, C. P. Lin, J. S. Schuman, W. G. Stinson, W. Chang, M. R. Hee, T. Flotte, K. Gregory, C. A. Puliafito, and J. G. Fujimoto, "Optical coherence tomography," *Science*, vol. 254, pp. 1178–1181, 1991.
- [7] A. F. Fercher, "Optical coherence tomography," *J. Biomedical Opt.*, vol. 1, pp. 157–173, 1996.
- [8] J. M. Schmitt, A. Knüttel, and R. F. Bonner, "Measurement of optical properties of biological tissues by low-coherence reflectometry," *Appl. Opt.*, vol. 32, pp. 6032–6042, 1993.
- [9] T. L. Lindmo, D. J. Smithies, Z. Chen, J. S. Nelson, and T. E. Milner, "Accuracy and noise in optical Doppler tomography," *Phys. Medicine Biol.*, vol. 43, pp. 3025–3044, 1998.
- [10] ———, "Monte Carlo simulation of optical coherence tomography and optical Doppler tomography," *SPIE*, to be published.
- [11] S. L. Gammill, K. B. Stapkey, and E. H. Himmellarb, "Roentgenology-pathology correlative study of neovasculature," *Am. J. Roentgenol.*, vol. 126, pp. 376–385, 1976.
- [12] J. R. Less, T. C. Skalak, E. M. Sevick, and R. K. Jain, "Microvascular architecture in a mammary carcinoma: Branching patterns and vessel dimensions," *Cancer Res.*, vol. 51, p. 265, 1991.
- [13] P. L. Carson, D. D. Adler, and J. B. Fowlkes, "Enhanced color flow imaging of breast cancer vasculature: Continuous wave Doppler and three-dimensional display," *J. Ultrasound Med.*, vol. 11, p. 77, 1992.
- [14] Z. Chen, T. E. Milner, X. J. Wang, S. Srinivas, and J. S. Nelson, "Optical Doppler tomography: Imaging *in vivo* blood flow dynamics following pharmacological intervention and photodynamic therapy," *Photochem. Photobiol.*, vol. 67, pp. 56–60, 1998.
- [15] J. K. Barton, A. J. Welch, and J. A. Izatt, "Investigating pulsed dye laser-blood vessel interaction with color Doppler optical coherence tomography," *Opt. Express*, vol. 3, p. 251, 1998.
- [16] S. Yazdanfar, M. D. Kulkarni, and J. A. Izatt, "High resolution imaging of *in vivo* cardiac dynamics using color Doppler," *Opt. Express*, vol. 1, p. 424, 1997.
- [17] A. Ichimiya, "Functional and structural brain imagings in dementia," *Psychiatry Clin Neurosci.*, vol. 52, pp. S223–S225, 1998.
- [18] R. D. Frostig, E. E. Lieke, D. Y. Ts'o, and A. Grinvald, "Cortical functional architecture and local coupling between neuronal activity and the microcirculation revealed by *in vivo* high-resolution optical imaging of intrinsic signals," in *Proc. Nat. Acad. Sci. USA*, vol. 87, pp. 6082–6086, 1990.
- [19] D. Kleinfeld, P. P. Mitra, F. Helmchen, and W. Denk, "Fluctuations and stimulus-induced changes in blood flow observed in individual capillaries in layers 2 through 4 of rat neocortex," *Proc. Nat. Acad. Sci. USA*, vol. 95, pp. 15741–15746, 1998.
- [20] S. N. Roper, M. D. Moores, G. V. Gelikonov, F. I. Feldchtein, N. M. Beach, M. A. King, V. M. Gelikonov, A. M. Sergeev, and D. H. Reitze, "In vivo detection of experimentally induced cortical dysgenesis in the adult rat neocortex using optical coherence tomography," *J. Neurosci Methods*, vol. 80, pp. 91–98, 1998.
- [21] L. Mandel and E. Wolf, *Optical Coherence and Quantum Optics*, Cambridge Univ. Press, 1995.
- [22] J. M. Schmitt, S. H. Xiang, and K. M. Yung, "Speckle in optical coherence tomography: A review," *J. Biomed. Opt.*, vol. 4, p. 95, 1999.



Zhongping Chen received the B.S. degree in applied physics from Shanghai Jiaotong University in 1982, an the M.S. degree in electrical engineering from Cornell University in 1987, and the Ph.D. degree in applied physics from Cornell University in 1992.

He joined Biological Component Corporation as the Director of Research in 1992 and managed corporate research between 1992–1993. In 1994, he was awarded a National Research Council Associate Fellowship at the Biotechnology Division of the U.S. Army Natick Research, Development, and Engineering Center. He joined Beckman Laser Beckman Laser Institute and Medical Clinic, University of California, Irvine in 1995 and is currently an Assistant Professor of Biomedical Engineering and Surgery at UCI. His research experience and interests are in the areas of biomedical imaging, photonic materials and devices, biomaterials, and biosensors. His current research foci are the investigation of light/tissue interactions, the development of optical and ultrasound technology for medical diagnosis and treatment, and the integration of advanced optical and semiconductor technology with biotechnology for the development of biomedical devices.



Yonghua Zhao was born in Zhejiang, China, in 1970. He received the B.S. degree in applied physics in Shanghai Jiao Tong University, and the Ph.D. degree from Shanghai Institute of Optics and Fine Mechanics, Chinese Academy of Science.

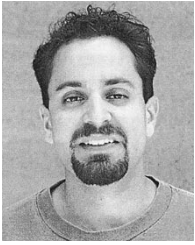
He is currently a Post-Doctoral Researcher at Beckman Laser Institute and Medical Clinic.



Shyam M. Srinivas received the B.S. degree in biomedical engineering from the University of California at San Diego in 1992. Currently he is in his sixth year in the Medical Scientist Training Program at the University of California, Irvine. This program confers both M.D. and Ph.D. degrees upon completion.

His Ph.D. study is being pursued in the Department of Electrical and Computer Engineering with his areas of interest being optical coherence tomography, polarization sensitive optical coherence tomography and optical Doppler tomography.

Mr. Srinivas is a student member of the Optical Society of America and SPIE, and is a finalist in the Association for the Advancement of Medical Instrumentation (AAMI) Young Investigator's Competition for 1999.



Neal Prakash received the B.A. degree in molecular and cellular biology with an emphasis in neurobiology from the University of California at Berkeley in 1992 and the Ph.D. degree in neurobiology and behavior from the University of California at Irvine in 1999.

He is currently enrolled in the University of California at Irvine Medical Scientist Training Program where he has been awarded an MSTP fellowship. He joined Prof. Ron D. Frostig's laboratory in 1994 and has been using the technique of intrinsic signal optical imaging to help merge the fields of molecular neurobiology and systems neurobiology. In 1997, he was awarded the American Heart Association fellowship to study regulation of blood flow in the brain. He is currently involved in several collaborations with the Beckman Laser Institute to help develop new high-resolution *in vivo* brain imaging techniques.

Ron D. Frostig, photograph and biography not available at the time of publication.